

# *D* MESON PRODUCTION AT CENTRAL RAPIDITY IN *pp* COLLISIONS AT 7 TeV WITH THE ALICE DETECTOR\*

GIAN MICHELE INNOCENTI

for the ALICE Collaboration

Department of Experimental Physics, University and INFN, Turin 10125, Italy

(Received December 7, 2011)

Heavy quark production is a powerful tool to test pQCD calculations in *pp* collisions in the new energy regime of the LHC. In addition, the measurement of the *D* meson  $p_t$  differential cross section provides a reference for the study of QCD matter effects on charm quarks in Pb–Pb collisions. Thanks to its excellent tracking system and particle identification capabilities, the ALICE detector allows charmed hadron measurements in the mid-rapidity region down to low momentum. We will present preliminary results for the  $p_t$  differential cross sections of  $D^0$ ,  $D^{*+}$  and  $D^+$  in *pp* collisions at 7 TeV measured via their hadronic decay channels. The status of the  $D_s^+$  and  $A_c$  analyses will also be presented.

DOI:10.5506/APhysPolBSupp.5.579

PACS numbers: 21.65.Qr, 21.65.Jk, 25.75 Cj

## 1. Introduction

The measurement of the charm production cross section in *pp* collisions allows to test in the new energy regime of the LHC the perturbative QCD calculations based on the factorization approach. Moreover, the *pp* results provide a crucial reference for Pb–Pb studies [1]. The first *pp* data at a centre-of-mass energy of 7 TeV were collected in March–September 2010. In these proceedings, the results for the  $D^0$ ,  $D^{*+}$ ,  $D^+$  and  $D_s^+$  analyses at 7 TeV reconstructed in the transverse momentum range  $2 < p_t < 12$  GeV/*c* at central rapidity ( $|y| < 0.5$ ) will be presented<sup>1</sup>. Results of the preliminary measurements at 2.76 TeV will also be shown.

---

\* Presented at the Conference “Strangeness in Quark Matter 2011”, Kraków, Poland, September 18–24, 2011.

<sup>1</sup> Shortly before the publication of these proceedings, the final results of the  $D^0$ ,  $D^{*+}$ ,  $D^+$  analysis in *pp* collisions at 7 TeV were presented [2]. They are in full agreement with the preliminary results reported here.

## 2. Detector layout and data sample

The ALICE apparatus [3] has excellent capabilities for open charm measurements. These analyses are performed using the tracking detectors and particle identification systems of the ALICE central barrel that covers the pseudo-rapidity region  $-0.9 < \eta < 0.9$  and is embedded in a magnetic field of  $B = 0.5$  T. The information from the central barrel detectors allows to track charged particles down to low transverse momenta ( $\approx 100$  MeV/ $c$ ) and provides charged hadron and electron identification as well as an accurate measurement of the positions of the primary and secondary (decay) vertices [4]. In this section, a brief description of the detectors utilized in these analyses will be given. The Time Projection Chamber (TPC) is the main tracking detector, providing track reconstruction and particle identification via the measurement of the specific energy deposit  $dE/dx$ . The Inner Tracking System (ITS) is the central barrel detector closest to the beam axis and is composed of six cylindrical layers of silicon detectors. The two innermost layers (at radii of  $\approx 4$  and  $7$  cm) are equipped with pixel detectors (SPD), the two intermediate layers (radii  $\approx 15$  and  $24$  cm) are made of drift detectors, while strip detectors are used for the two outermost layers (radii  $\approx 39$  and  $44$  cm). The ITS plays a central role in detecting secondary vertices originating from open charm decays because it allows the measurement of the track impact parameter with a resolution better than  $50$   $\mu\text{m}$  for tracks with  $p_t > 1.3$  GeV/ $c$  [2]. The Time-of-Flight (TOF) detector is used for pion, kaon and proton identification on the basis of their Time of Flight. The TOF measurement provides kaon/pion separation up to a momentum of about  $1.5$  GeV/ $c$ . All the three detectors have full azimuthal coverage. The data sample used for these analyses has been collected during the 2010 LHC run with  $pp$  collisions at  $7$  TeV and it consists of  $\approx 100$  million minimum-bias events for  $D^0$ ,  $D^{*+}$ ,  $D^+$  (integrated luminosity  $L_{\text{int}}$  of  $1.6$  nb $^{-1}$ ) and  $\approx 300$  million minimum-bias events for the  $D_s^+$  meson ( $L_{\text{int}} = 4.8$  nb $^{-1}$ ). Proton-proton collisions at lower energy  $\sqrt{s} = 2.76$  TeV were also analyzed in order to have a cross-check for the reference of the Pb-Pb studies [1]. The minimum-bias trigger was based on the SPD and VZERO detectors. The latter is made of two scintillator hodoscopes positioned in the forward and backward regions of the experiment [3].

## 3. $D$ meson production measurements in ALICE

The production of  $D^0$ ,  $D^{*+}$ ,  $D^+$  and  $D_s^+$  was measured in  $pp$  collisions at  $7$  TeV in the central rapidity region via the exclusive reconstruction of their hadronic decays. The decay channels with their branching ratios are:  $D^0 \rightarrow K^-\pi^+$  (BR =  $3.89 \pm 0.05\%$ ),  $D^{*+} \rightarrow D^0\pi^+$  (strong decay with BR =  $67.7 \pm 0.5\%$ ),  $D^+ \rightarrow K^-\pi^+\pi^+$  (BR =  $9.4 \pm 0.4\%$ ),

$D_s^+ \rightarrow K^+K^-\pi^+$  (BR =  $5.49 \pm 0.27\%$ ) [5]. Other analyses are currently under way:  $D^0 \rightarrow K^-\pi^+\pi^-\pi^+$ ,  $\Lambda_c^+ \rightarrow pK^-\pi^+$ ,  $\Lambda_c^+ \rightarrow K_s^0p$  and  $\Lambda_c^+ \rightarrow \Lambda p$ . The analysis strategy for the extraction of the signals out of the large combinatorial background is based on the reconstruction and selection of secondary vertex topologies with significant separation from the primary vertex (typically a few hundred micrometers). The  $D$  meson candidates are built starting from track combinations with proper charges and selected according to topological cuts. Single tracks are previously selected with respect to their momentum and pseudorapidity ( $p_t > 0.4$  GeV/ $c$  and  $|\eta| < 0.8$ ) and to quality cuts. In the case of  $D^0$  mesons, the two main cut variables are the product of the impact parameters of the kaon and of the pion ( $d_0^K \times d_0^\pi$ ) and the cosine of the pointing angle ( $\theta_{\text{pointing}}$ ) that is the angle between the reconstructed  $D$  meson momentum and the line which connects the primary and secondary vertices. The selection on the pointing angle is also used for  $D^+$  and  $D_s^+$  together with a cut on the distance between the reconstructed primary and secondary vertices. The  $D^{*+}$  analysis exploits the narrow signal in the difference between the invariant masses of the three final state hadrons and of the two  $D^0$  decay prongs. A particle identification (PID) strategy which combines the TPC and TOF information has also been adopted for the pions and the kaons: the PID selection provides further background rejection while preserving most of the  $D$  meson signal. For the  $D_s^+$  meson, the decay into the  $K^+K^-\pi^+$  final state occurs via resonant channels with a  $\phi$  or a  $K^{0*}$  meson in the intermediate state. In the present analysis, the decay  $D_s^+ \rightarrow \phi\pi^+ \rightarrow K^+K^-\pi^+$  was selected by requiring that one of the two pairs of opposite-signed tracks has invariant mass compatible with the  $\phi$  mass and PID information for both particles compatible with the kaon hypothesis. In order to extract the signal, the invariant mass distributions of the candidates are fit with a function that consists of a Gaussian term describing the signal and an exponential term for the background. In the  $D^{*+}$  case, the background shape has been fit with a power law with threshold at the mass of the pion, convoluted with an exponential [6]. Figure 1 (left) shows the invariant mass distribution of  $D_s^+$  candidates in the transverse momentum range  $4 < p_t < 6$  GeV/ $c$  obtained from the analysis of  $\approx 300$  million minimum bias events. The measured inclusive raw yields obtained from the invariant mass analysis in each  $p_t$  bin has been corrected for acceptance (which also considers the rapidity range of the cross section measurement  $|y| < 0.5$ ) and selection efficiency of prompt  $D$  mesons using Monte Carlo simulations based on the PYTHIA 6.4.21 event generator [7] with Perugia-0 tuning [8]. The correction factor that accounts for the feed-down from  $B$  meson decays has been evaluated using the Monte Carlo efficiency for feed-down  $D$  mesons and the FONLL pQCD calculation which well describes bottom production at Tevatron [9] and at the LHC [10, 11]. The feed-down fraction is 10–15%

depending on the  $p_t$  of the  $D$  meson. Figure 1 (right) shows the efficiency for the  $D_s^+$  meson with  $|y| < 0.5$  as a function of the transverse momentum  $p_t$  for prompt  $D$  mesons and  $D$  mesons from  $B$  feed-down decays.

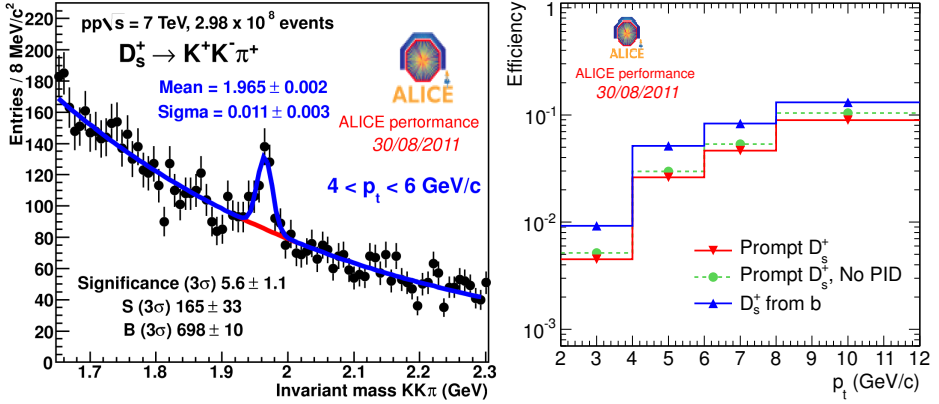


Fig. 1. Left: Invariant mass distribution of  $D_s^+$  candidates in the transverse momentum range  $4 < p_t < 6$  GeV/ $c$  obtained from the analysis of  $\approx 300$  million minimum bias events. Right: Efficiency for the  $D_s^+$  meson as a function of  $p_t$  for prompt  $D$  mesons (with and without PID selection) and  $D$  mesons from  $B$  feed-down.

## 4. Results

The  $p_t$  differential cross sections obtained for prompt  $D^0$ ,  $D^{*+}$ ,  $D^+$  mesons are shown in Fig. 2 compared to two theoretical predictions, namely FONLL [9] and GM-VFNS [12]: the measurements are well described by both the calculations within the uncertainties.

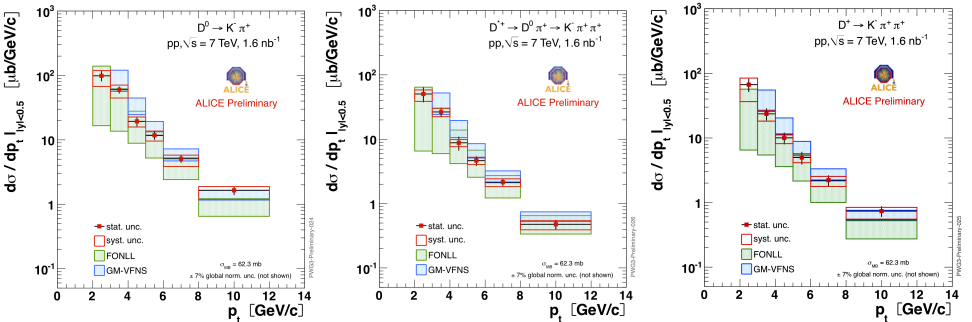


Fig. 2. Preliminary  $D^0$ ,  $D^{*+}$ ,  $D^+$   $p_t$  differential cross section measured with an integrated luminosity of  $1.6$  nb $^{-1}$  ( $\approx 100$  million minimum-bias events) in the  $p_t$  range 2–12 GeV/ $c$  compared to pQCD predictions (see the text for details).

In Fig. 3 (left) the  $p_t$  differential cross section obtained for prompt  $D_s^+$  mesons is shown: a theoretical prediction for the  $D_s^+$  meson is not yet available. In the central panel of Fig. 3, the ratios between the  $D$  meson cross sections integrated in the  $p_t$  range  $2 < p_t < 12$  GeV/ $c$  ( $D^0/D^+$ ,  $D^0/D^{*+}$ ,  $D^0/D_s^+$  and  $D^+/D_s^+$ ) measured by ALICE are compared with the results of other experiments, namely LHCb [13],  $e^+e^-$  data [14], H1 [15]: ALICE results are compatible with the other measurements within the uncertainties.

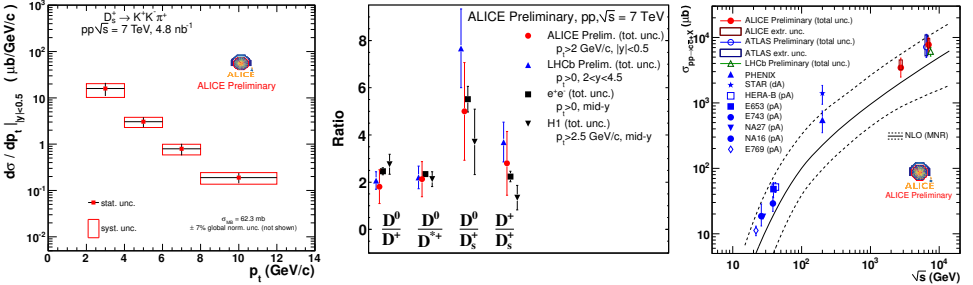


Fig. 3. Left: Preliminary  $D_s^+$   $p_t$  differential cross section measured with an integrated luminosity of  $4.8 \text{ nb}^{-1}$  ( $\approx 300$  million minimum-bias events) in the  $p_t$  range 2–12 GeV/ $c$ . Center: Ratios between the  $D$  meson cross sections integrated in the  $p_t$  range  $2 < p_t < 12$  GeV/ $c$  measured by ALICE compared with the results from other experiments [13, 15, 14]. Right: Total charm production cross section as a function of the collision energy measured by different experiments compared with the next-to-leading order predictions. Total uncertainties are shown.

The production cross sections for prompt  $D$  mesons were extrapolated in the full kinematical phase space (down to  $p_t = 0$  GeV/ $c$  and to the full  $y$  coverage) using FONLL calculations [9]. The total charm production cross section was extracted by dividing each  $D$  meson production cross section by its fragmentation ratio, which represents the relative probability of a charm quark to fragment into a specific hadron species. For these results, the fragmentation ratios measured at LEP [14, 16] have been used. The final results is obtained by combining the measurements of the total charm production cross section of  $D^0$ ,  $D^{*+}$  and  $D^+$ .

The total charm production cross section as a function of the collision energy is shown in the right panel of Fig. 3. ALICE results for  $pp$  collisions at 7 TeV and at 2.76 TeV are shown together with the measurements of ATLAS, LHCb [17, 13] and other experiments at different energies [18, 19, 20]. The black curves show the next-to-leading-order predictions from the MNR calculation [21] and its uncertainties: the measurements are in good agreement with the theoretical prediction over three order of magnitudes.

## 5. Conclusions

The preliminary measurements of the production cross sections of prompt  $D$  mesons in  $pp$  collisions at  $\sqrt{s} = 7$  TeV in the central rapidity region and in the range  $2 < p_t < 12$  GeV/ $c$  have been presented.  $D$  mesons were reconstructed in the ALICE detector via their hadronic decay channels  $D^0 \rightarrow K^- \pi^+$ ,  $D^{*+} \rightarrow D^0 \pi^+$ ,  $D^+ \rightarrow K^- \pi^+ \pi^+$  and  $D_s^+ \rightarrow K^+ K^- \pi^+$ . The  $p_t$  differential cross sections are well described within the uncertainties by perturbative QCD theoretical calculations, namely FONLL [9] and GM-VFNS [12]. These results have been used as a reference for the Pb–Pb studies after scaling to the proper energy [1].

## REFERENCES

- [1] A. Grelli [ALICE Collaboration], *Acta Phys. Pol. B Proc. Suppl.* **5**, 585 (2012), this issue.
- [2] K. Aamodt *et al.* [ALICE Collaboration], [arXiv:1111.1553 \[hep-ex\]](#), submitted for publication to *J. High Energy Phys.*
- [3] K. Aamodt *et al.* [ALICE Collaboration], *JINST* **3**, S08002 (2008).
- [4] A. Rossi *et al.* [ALICE Collaboration], *PoS (Vertex2010)*, 017 (2001) [[arXiv:1101.3491v1 \[physics.ins-det\]](#)].
- [5] K. Nakamura *et al.* [Particle Data Group], *J. Phys. G* **37**, 075021 (2010).
- [6] D. Acosta *et al.* [CDF Collaboration], *Phys. Rev. Lett.* **91**, 241804 (2003).
- [7] T. Sjostrand, S. Mrenna, P. Skands, *J. High Energy Phys.* **05**, 026 (2006).
- [8] P.Z. Skands, [arXiv:0905.3418 \[hep-ph\]](#).
- [9] M. Cacciari *et al.*, *J. High Energy Phys.* **0407**, 033 (2004); private communication.
- [10] R. Aaij *et al.* [LHCb Collaboration], *Phys. Lett.* **B694**, 209 (2010).
- [11] V. Khachatryan *et al.* [CMS Collaboration], *Eur. Phys. J.* **C71**, 1575 (2011) [[arXiv:1011.4193v1 \[hep-ex\]](#)].
- [12] B.A. Kniehl *et al.*, *Phys. Rev. Lett.* **96**, 012001 (2006).
- [13] LHCb Collaboration, internal note: LHCb-CONF-2010-013 (2010).
- [14] L. Gladilin, [arXiv:hep-ex/9912064](#).
- [15] ZEUS Collaboration, *J. High Energy Phys.* **07**, 074 (2007).
- [16] K. Ackerstaff *et al.* [OPAL Collaboration], *Eur. Phys. J.* **C1**, 439 (1997).
- [17] ATLAS Collaboration, internal note: ATLAS-CONF-2011-017 (2011).
- [18] C. Lourenco, H.K. Wohri, *Phys. Rep.* **433**, 127 (2006).
- [19] J. Adams *et al.* [STAR Collaboration], *Phys. Rev. Lett.* **94**, 62301 (2005).
- [20] A. Adare *et al.* [PHENIX Collaboration], [arXiv:1005.1627 \[nucl-ex\]](#).
- [21] M. Mangano, P. Nason, G. Ridolfi, *Nucl. Phys.* **B373**, 295 (1992).